ELSEVIER

Photoinduced electron transfer in supramolecular assemblies of transition metal complexes

Itamar Willner [a,*], Evgeny Kaganer [a], Ernesto Joselevich [a], Heinz Dürr [b],
Elke David [b], Maxwell J. Günter [c], Martin R. Johnston [c]

[a] *Institute of Chemistry and Farkas Center for Light-Induced Processes,
The Hebrew University of Jerusalem, Jerusalem 91904, Israel*
[b] *Universität des Saarlandes, Organische Chemie, Fachbereich 11.2, 66041 Saarbrücken,
Germany*
[c] *Department of Chemistry, The University of New England, Armidale, NSW 2351, Australia*

Contents

Abstract

Photoinduced electron transfer in supramolecular assemblies consisting of π-donor dialk-oxyarene-functionalized photosensitizers and bipyridinium electron acceptors is examined. The photosensitizers include Ru(II)-tris-bipyridine complexes tethered by multi-branch one-

---

* Corresponding author. Fax: (+972) 2 6527715; e-mail: willnea@vms.huji.ac.il

shell and two-shell dialkoxybenzene π-donor sites or a Zn(II)-porphyrin capped by a dialkoxy-benzene receptor site. The photosensitizer/electron-acceptor supramolecular complexes behave as non-covalent diads and polyads. Effective internal electron transfer quenching within the supramolecular assemblies proceeds. A quantitative model that accounts for the photoinduced electron transfer in the systems is formulated. © 1998 Elsevier Science S.A.

1. Introduction

The photosynthetic reaction center represents an evolutionary optimized organized assembly where vectorial photoinduced electron transfer (ET) leads to effective charge separation [1–3]. Substantial research efforts have been directed to mimic functions of natural photosynthesis and to tailor artificial photosynthetic systems [4–6]. Photoinduced ET in microheterogeneous reaction media, such as micelles [7–9], charged colloids [10,11] or water-in-oil microemulsion [12–15], led to effective charge separation of the ET products. Coupling of homogeneous catalysts [16–19], heterogeneous catalysts [20–22] or enzymes [23–28] to the photogenerated redox products led to light-stimulated chemical transformations such as H_2-evolution and CO_2-fixation.

One of the methods of mimicking the vectorial ET and charge separation in the photosynthetic reaction center includes the synthesis of covalently linked photosensitizer–acceptor diads [29,30], or donor–photosensitizer–acceptor triads [31–40] and pentads [41,42], exhibiting the appropriate redox-potential ordering for vectorial ET. Effective stabilization of the photogenerated ET products against back reaction was accomplished by their spatial separation in the molecular arrays. This concept was further developed by the organization of molecular assemblies in heterogeneous matrices such as zeolites [43] or layered phosphates [44,45]. The structural alignment and rigidification of the molecular assemblies in these systems leads to effective charge separation. Recently, we have been active in developing novel concepts for organizing molecular and macromolecular donor–acceptor diad assemblies that mimic functions of the photosynthetic reaction center [46–49]. One approach is based on the assembly of supramolecular complexes consisting of photosensitizer–acceptor diads [49], and polyads [47,48] stabilized by non-covalent interactions between the electron acceptor and a multi-receptor-functionalized photosensitizer.

2. Photoinduced ET in polydentate receptor-functionalized photosensitizer/electron-acceptor supramolecular assemblies

The approach to organize "octopus-like" supramolecular assemblies between a receptor-functionalized photosensitizer and electron acceptors for controlled photo-

induced ET is schematically shown in Fig. 1. Specific affinity of the electron acceptor to the receptor sites results in supramolecular complexes of variable stoichiometries and efficient intra-complex ET quenching. Provided the reduced photoproduct lacks affinity for the receptor site, intimate back ET competes with the charge separation of the photogenerated redox-species.

2.1. Kinetic model and analysis

A detailed kinetic model that accounts for the photoinduced ET in such supramolecular assemblies has been formulated [47]. The parallel and consecutive reactions

(a)
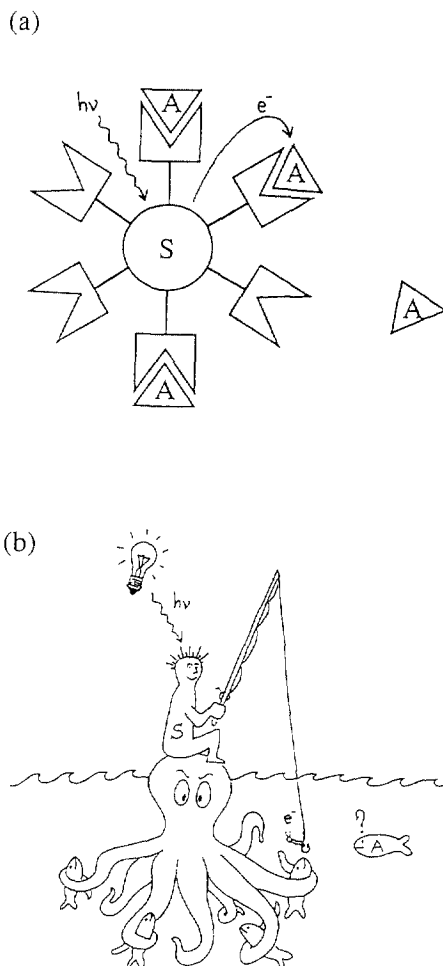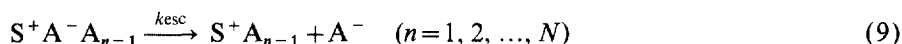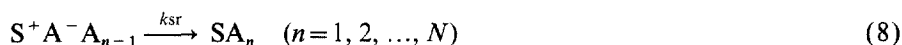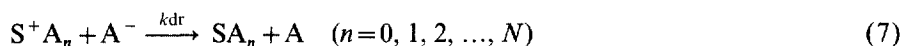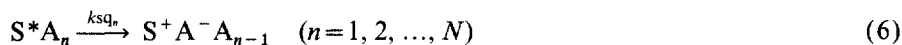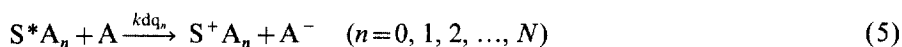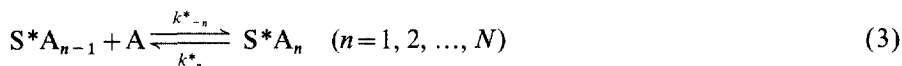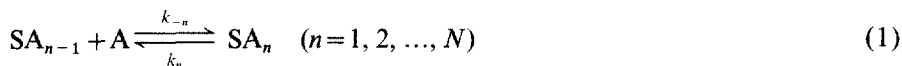

(b)

Fig. 1. (a) Schematic representation of the approach of organizing octopus-like supramolecular assemblies between a receptor-functionalized photosensitizer and electron acceptors for controlled photoinduced ET. (b) A free representation.

occurring in these supramolecular complexes are summarized in Eqs. (1)–(9).

$$SA_{n-1} + A \underset{k_n}{\overset{k_{-n}}{\rightleftharpoons}} SA_n \quad (n = 1, 2, ..., N) \tag{1}$$

$$SA_n \xrightarrow{hv} S^*A_n \quad (n = 0, 1, 2, ..., N) \tag{2}$$

$$S^*A_{n-1} + A \underset{k^*_n}{\overset{k^*_{-n}}{\rightleftharpoons}} S^*A_n \quad (n = 1, 2, ..., N) \tag{3}$$

$$S^*A_n \xrightarrow{kD_n} SA_n \quad (n = 0, 1, 2, ..., N) \tag{4}$$

$$S^*A_n + A \xrightarrow{kdq_n} S^+A_n + A^- \quad (n = 0, 1, 2, ..., N) \tag{5}$$

$$S^*A_n \xrightarrow{ksq_n} S^+A^-A_{n-1} \quad (n = 1, 2, ..., N) \tag{6}$$

$$S^+A_n + A^- \xrightarrow{kdr} SA_n + A \quad (n = 0, 1, 2, ..., N) \tag{7}$$

$$S^+A^-A_{n-1} \xrightarrow{ksr} SA_n \quad (n = 1, 2, ..., N) \tag{8}$$

$$S^+A^-A_{n-1} \xrightarrow{kesc} S^+A_{n-1} + A^- \quad (n = 1, 2, ..., N) \tag{9}$$

The photosensitizer S functionalized by N receptor sites, forms ground-state supramolecular complexes of variable stoichiometries, SA_n ($n = 0, 1, 2, ..., N$), Eq. (1). Photoexcitation of the supramolecular complexes yields characteristic association and dissociation features of the excited assemblies, Eqs. (2) and (3). The photoexcited photosensitizers in the respective complexes undergo natural decay, Eq. (4), diffusional ET by the solution-solubilized electron acceptor, Eq. (5), and intramolecular, static, ET-quenching in the respective supramolecular complexes, Eq. (6). The photogenerated redox species resulting from the different quenching routes can then undergo diffusional recombination, Eq. (7), intramolecular back ET, Eq. (8), or separation of the intimate complex of photoproducts leading to charge-separated redox species, Eq. (9). The kinetic model formulated assumes that the diffusional quenching rate is proportional to the electron acceptor concentration, where the static ET quenching rate is proportional to the stoichiometry of the supramolecular complexes. The supramolecular assemblies SA_n are found in equilibrium prior to excitation and their concentrations, which follow a standard binomial distribution, are given by Eq. (10), where S_o is the analytical concentration of the multireceptor photosensitizer, N is the number of receptor sites or the maximal stoichiometry, and K is the association constant between the receptor site and the electron acceptor. Photoexcitation of the system yields equal fractions of every supramolecular configuration, and their distribution, immediately upon excitation,

is identical to the ground-state distribution. As the photosensitizers in the different complexes decay at different rates, the overall decay of the photoexcited state is expected to be multiexponential. The decay of the excited state according to this model is given by Eq. (11), where $I(0)$ is the excited state concentration, or the luminescence emission intensity, immediately after the excitation, k_{dq} is the diffusional ET quenching rate constant for all excited photosensitizer populations, and k_{sq} is the first-order, static, ET-quenching rate constant of the photosensitizer by a single electron acceptor unit. Note that the ET quenching rate constant of the supramolecular complex of stoichiometry SA_n is nk_{sq}.

$$[SA_n] = \frac{S_o}{(1+K[A])^N} \frac{N!}{n!(N-n)!} K^n[A]^n \quad (n=0, 1, 2,..., N) \tag{10}$$

$$I(t) = I(0) \, e^{-(k_D+k_{dq}[A])t} \left(\frac{1+K[A] \, e^{-k_{sq}t}}{1+K[A]} \right)^N \tag{11}$$

Since the static quenching is significantly faster than the diffusional ET-quenching $(k_{sq} \gg k_{dq}[A])$, the decay of the excited state, or the luminescence, Eq. (11), is composed of a fast decay that originates from intra-complex quenching and a slow decay that originates from the native decay and the diffusional quenching processes. Thus, the slow decay can be extracted from Eq. (11), assuming $K[A] \, e^{-k_{sq}t}$ is negligible, and is given by Eq. (12).

$$I_{slow}(t) = I(0) \frac{1}{(1+K[A])^N} \, e^{-(k_D+k_{dq}[A])t} \tag{12}$$

The steady-state luminescence of the photosensitizer at any concentration of the quencher is proportional to the integration over time of the transient luminescence, Eq. (11). Since, however, the term $K[A] \exp(-k_{sq}t)$ related to the intramolecular quenching decays fast and quickly becomes negligible, its contribution to the integration over time is small. Thus, the luminescence intensities of the photosensitizer in the absence of a quencher (I_o) and in the presence of the electron acceptor (I) are given by Eq. (13), where τ_o is the natural lifetime of the photosensitizer and τ is given by Eq. (14).

$$\frac{I_o}{I} = (1+K[A])^N \frac{\tau_o}{\tau} \tag{13}$$

$$\frac{1}{\tau} = k_D + k_{dq}[A] \tag{14}$$

By rearranging Eqs. (13) and (14), a modified Stern–Volmer expression, outlined in Eq. (15), can be derived. Note that this theoretical consideration, Eq. (13), implies that the relation I_o/I as a function of the electron-acceptor concentration is non-

linear as the term $(1 + K[A])^N$ is a polynomial of degree N.

$$\left(\frac{I_o}{I}\frac{\tau}{\tau_o}\right)^{1/N} = 1 + K[A] \tag{15}$$

This kinetic model applies for supramolecular photosensitizer–electron acceptor assemblies of any variable stoichiometry and any affinity interactions leading to non-covalent, dynamically labile, association. This interaction could be H-bonds, π-donor–acceptor interactions, hydrophobic association, etc. We have applied this model to analyze the photoinduced ET processes in a series of supramolecular complexes formed between photosensitizers functionalized by multi-receptor π-donor sites and 4,4'-bipyridinium electron acceptors [47,48]. We will address here the application of this model in analyzing the photochemically induced ET processes in two series of supramolecular assemblies, and discuss the methods of tailoring supramolecular structures exhibiting effective ET-quenching and charge separation.

N,N'-Dialkyl-4,4'-bipyridinium salts form π-donor–acceptor complexes with electron-rich aromatic compounds [50–54]. Specifically, complexes between dialkoxybenzenes and 4,4'-bipyridinium salts, or the bipyridinium cyclophane, cyclo[bis(N,N'-p-xylylene-4,4'-bipyridinium), BXV^{4+}, (**1**), have been extensively characterized [55–57].
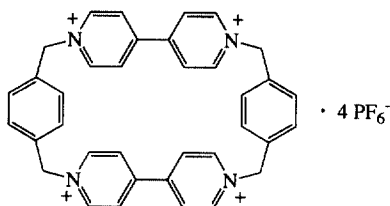
1

Accordingly, the photoinduced ET reactions in supramolecular complexes formed between photosensitizers functionalized by π-donor dialkoxybenzene, functionalized photosensitizers, and bipyridinium salts were examined. The first system, that will be discussed in detail, includes a comparison of the photoinduced ET reactions occurring in supramolecular assemblies formed between multi-receptor Ru(II)-tris-bipyridine complexes functionalized by π-donor–dialkoxybenzene units and the bipyridinium cyclophane, BXV^{4+}. The photosensitizers include the one-shell photosensitizer tris(4,4'-bis[3,6-dioxa-1-octyloxy-methylene]-2,2'-bipyridine)-ruthenium(II) chloride, (**2**), where six dialkoxybenzene units are tethered in a single-shell configuration to the central Ru(II)-photosensitizer, and tris(4,4'-bis[3,6-dioxa-8-(4-(3,6-dioxa-8-anisoxy)oxyloxy)phenylenoxy-1-octyloxy-methylene]-2,2'-bipyridine)-ruthenium(II) dichloride, (**3**), that includes 12 dialkoxybenzene receptor units in a two-shell configuration.

2
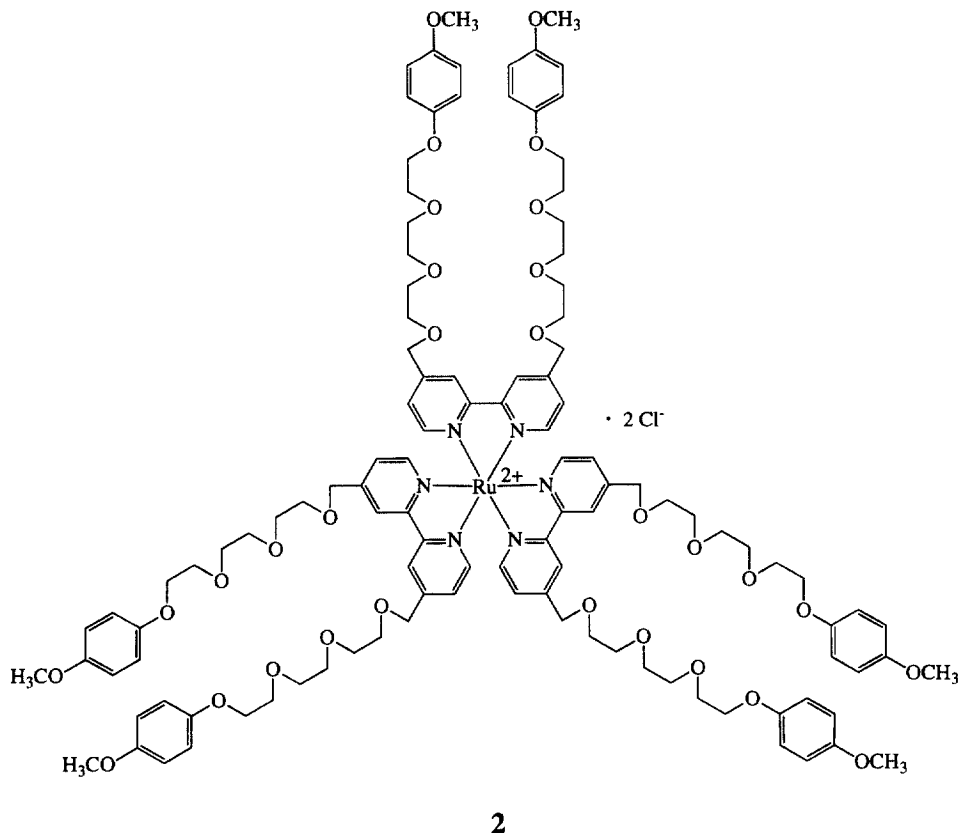
2.2. Steady-state emission experiments

Fig. 2 shows the steady-state luminescence quenching of (**2**) and (**3**) by BXV^{4+}. Non-linear Stern–Volmer plots are obtained and the deviation from linearity is pronounced for photosensitizer (**3**). Control experiments that employed photosensitizers lacking the dialkoxybenzene receptor sites revealed linear Stern–Volmer quenching plots in the presence of BXV^{4+}. Thus, the non-linearity of the steady-state luminescence quenching of the π-donor dialkoxybenzene-functionalized photosensitizers by BXV^{4+} is consistent with a complex ET-quenching route involving static and diffusional quenching of the excited state.

2.3. Transient emission experiments

Fig. 3(A) and (B) show the transients of the luminescence decay of (**2**) and (**3**), respectively, in the presence of different concentrations of BXV^{4+}. The luminescence decay curves reveal two important features: the initial luminescence intensity decreases as the concentration of BXV^{4+} increases, and the luminescence lifetime is
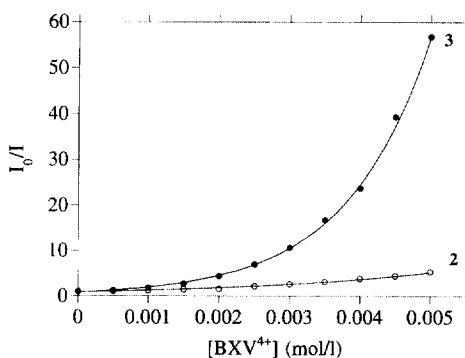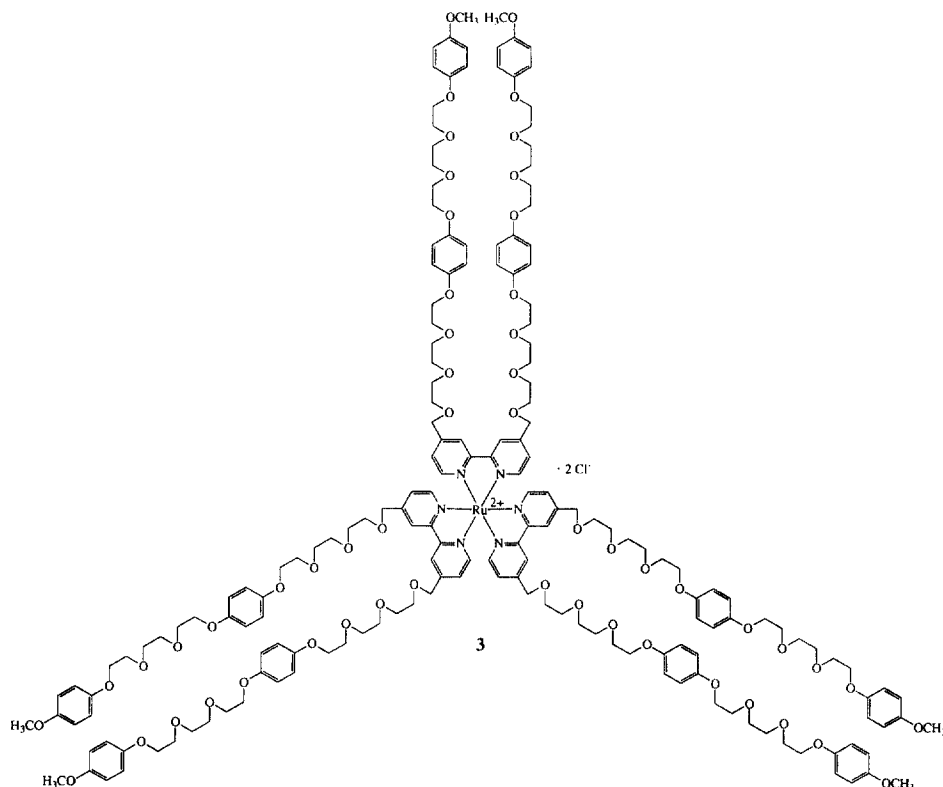
Fig. 2. Stern–Volmer plots for the steady-state luminescence quenching of **2** and **3** by BXV^{4+}. The two photosensitizers are at a concentration of 4.5×10^{-5} M.

shortened upon increasing the concentration of BXV^{4+}. These observations are consistent with the kinetic model derived for the photoinduced ET quenching routes in the multi-receptor functionalized photosensitizers and BXV^{4+} supramolecular complexes. Upon increasing the BXV^{4+} concentration, the fraction of supramolecu-

A

B

Fig. 3. Transient luminescence intensities of (A) **2**, and (B) **3**, in the presence of BXV^{4+}. Upper curves corres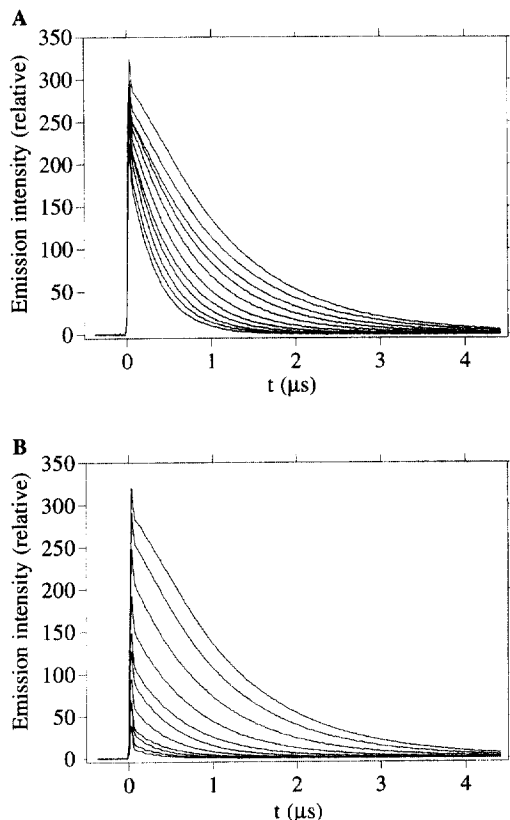pond to the photosensitizer luminescence without BXV^{4+}. All other transients represent the systems with added BXV^{4+} at consecutive increments of 5×10^{-4} up to an overall concentration of 5.0×10^{-3} M.

lar π-donor–acceptor complexes increases, and hence intramolecular, static quenching is enhanced. This is accompanied by a fast decay component in transient luminescence intensity, see Eq. (11), and is reflected by the decrease in the initial luminescence intensity. The shortening in the luminescence lifetime upon addition of BXV^{4+}, originates from the diffusional ET-quenching of the excited photosensitizers by BXV^{4+} and corresponds to the slow component in the transient luminescence decay, Eq. (12).

Comparison of the effects of added BXV^{4+} on the luminescence transients of the one-shell and two-shell π-donor photosensitizers reveal significant differences that cannot be rationalized in terms of a simple increase in the number of π-donor–receptor sites. For example, at a BXV^{4+} concentration of 5.0×10^{-3} M the initial luminescence intensity of (**2**) decreases to ca. 30%, whereas ca. 95% of the initial luminescence of (**3**) is quenched. Control experiments revealed that for poly-oxyethylene-tethered Ru(II)-tris-bipyridine complexes lacking the π-donor dialkoxy-
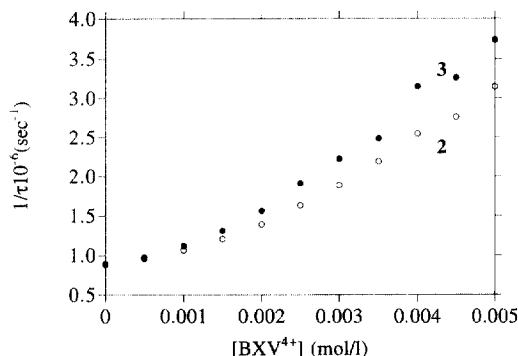
Fig. 4. Shortening of the lifetime of the slow luminescence decay of **2** and **3** at different concentrations of BXV^{4+}. Data extracted from Fig. 3.

benzene sites, no decrease in the initial luminescence intensity is observed upon addition of BXV^{4+}, but only the luminescence lifetime decreases. These control experiments support the fact that the decrease in the initial luminescence intensity originates from the fast, static, intramolecular quenching of the excited photosensitizer by BXV^{4+} units associated with the dialkoxybenzene sites and stabilized by π-donor–acceptor interactions.

Fig. 4 shows the shortening of the luminescence lifetimes of the photosensitizers (**2**) and (**3**) upon addition of variable concentrations of BXV^{4+}. The diffusional ET rate constants k_{dq} were calculated from these plots using Eq. (14). The diffusional ET-quenching rates for the two photosensitizers are almost identical.

2.4. Supramolecular association and stoichiometry analysis

Fig. 5(A) and 5(B) show the modified Stern–Volmer analysis of the steady-state luminescence quenching of the photosensitizers (**2**) and (**3**) upon addition of BXV^{4+}, specifically according to Eq. (15), assuming different maximal supramolecular stoichiometry of $N = 1$ and $N = 6$. It is evident that linear relationships are obtained upon assuming maximal supramolecular stoichiometries of $N = 6$ for both photosensitizers (**2**) and (**3**). That is, even though photosensitizer (**3**) includes 12 π-donor binding sites for BXV^{4+}, the photosensitizer provides only six receptor sites for the formation of supramolecular complexes. The slope of the modified Stern–Volmer plots corresponds to the association constant of the electron-acceptor to the π-donor site. We find that for photosensitizer (**2**) the association constant of a dialkoxybenzene unit, or π-donor branch to BXV^{4+}, is $K = 20 \pm 4 \ M^{-1}$. The derived association constant of a π-donor branch of the two-shell photosensitizer is, however, $K = 110 \pm 10 \ M^{-1}$. The derived association constants can be used to calculate the fractions of the various supramolecular stoichiometries at any BXV^{4+} concentration using Eq. (10).

Fig. 6(A) and 6(B) show the histograms representing the distribution of supramolecular photosensitizer–BXV^{4+} complexes of variable stoichiometries for (**2**) and
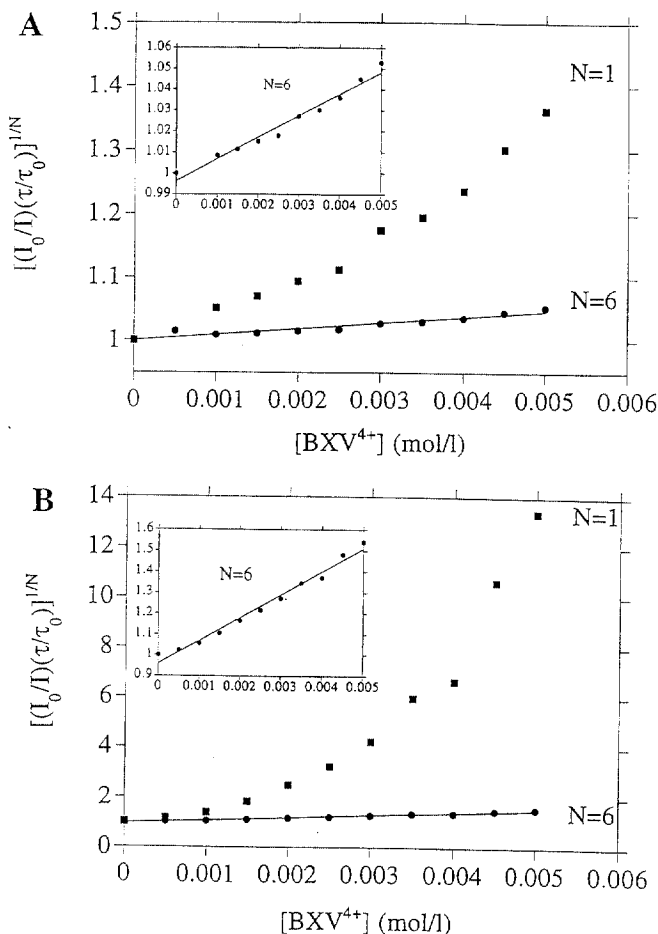
Fig. 5. Modified Stern–Volmer plots for the luminescence quenching of (A) **2** and (B) **3** by BXV^{4+}, assuming different maximal supramolecular stoichiometries. Linear fitting is observed for both when $N = 6$ (vertical zoom inset).

(**3**) respectively. These histograms are derived for the photosensitizer concentration, 4.5×10^{-5} M, and BXV^{4+}, 5.0×10^{-3} M, using Eq. (10) and the respective association constants. The one-shell photosensitizer, (**2**), is mostly in a free configuration (ca. 75%); about 20% of the photosensitizer is bound to one BXV^{4+} unit and a very low portion has a supramolecular stoichiometry of $n = 2$. The population of higher stoichiometries at this BXV^{4+} bulk concentration is negligible. The histogram of (**3**), however, reveals substantially different results. Only 7% of the photosensitizer exists in the unbound configuration, whereas the supramolecular configuration that includes two BXV^{4+} units bound to the chromophore is the highest population, and supramolecular complexes with the stoichiometries $n = 1$ and $n = 3$ complete most of the supramolecular structures. The histogram for (**3**), Fig. 6(B), also reveals
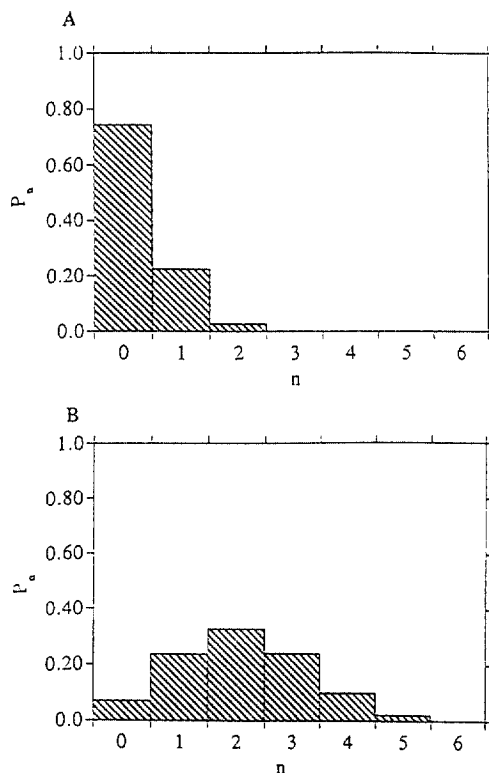
Fig. 6. Histograms representing the equilibrium statistical distribution of stoichiometries of the supramolecular assemblies formed by (A) **2** and (B) **3** in the presence of BXV^{4+} (5.0×10^{-3} M), according to Eq. (10) and calculated values of K.

that significant populations of $n = 4$ and $n = 5$ coexist in this dynamic exchangeable system.

The analysis of the photoinduced ET in the π-donor-functionalized photosensitizers reveals, for the two-shell photosensitizer (**3**), a substantially higher affinity to form supramolecular complexes between the dialkoxybenzene sites and BXV^{4+} than with the one-shell photosensitizer, (**2**). This is reflected by the higher association constant of BXV^{4+} to the dialkoxybenzene branch and the fact that the photosensitizer (**3**) exists (>93%) in supramolecular structures of variable stoichiometries with BXV^{4+}. The higher binding affinity of BXV^{4+} to the two-shell photosensitizer is attributed to a cooperative binding of the two dialkoxybenzene units to BXV^{4+}, forming a π-stacked supramolecular complex, Fig. 7. Indeed, previous studies showed that the association of the 4,4'-bipyridinium electron acceptor to a bis-dialkoxybenzene cyclophane is enhanced compared with the binding affinity of the bipyridinium salt to dialkoxybenzene [58–60]. Also, the successful synthesis of bis-dialkoxybenzene cyclophane/BXV^{4+} catenanes [61–63] was attributed to the favored intermediary formation of a π-stacked supramolecular complex between the bis-
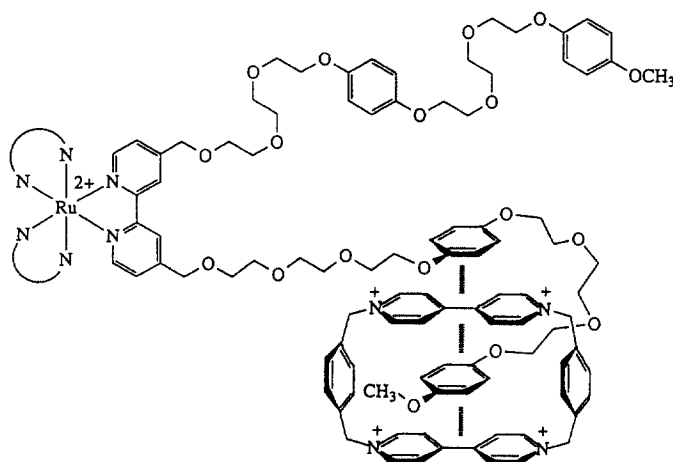
Fig. 7. Schematic structure for the cooperative binding of BXV^{4+} by two adjacent dialkoxybenzene units of one branch of the two-shell multireceptor photosensitizer **3**. The upper branch is free and the lower one binds BXV^{4+} units.

dialkoxybenzene unit and BXV^{4+}. The formation of the π-stacked complex between the two-shell branch and BXV^{4+} explains nicely the derived maximal stoichiometry of the supramolecular complex between (**3**) and BXV^{4+} that was found to correspond to $N=6$. Thus, although (**3**) includes 12 π-donor association sites, the maximal stoichiometry, or available receptor sites, is six. This is consistent with the participation of two dialkoxybenzene units as a single binding site for BXV^{4+} in the form of a π-stacked configuration.

2.5. Internal ET analysis

The high affinity of BXV^{4+} for the two-shell photosensitizer yields high populations of supramolecular complexes of variable stoichiometries. This results in efficient intramolecular ET quenching that was reflected by a decrease in the initial intensity of the luminescence that was attributed to a fast decay of the excited photosensitizer via a static, intramolecular ET-quenching route. This explanation is confirmed by following the luminescence intensity of the photosensitizers (**2**) and (**3**) at substantially shorter time scales. Fig. 8(A) and 8(B) show the transient decay curves of (**2**) and (**3**) at different concentrations of BXV^{4+} and at a nanosecond time-window. A fast luminescence decay component, with enhanced intensity upon increase of BXV^{4+} concentration, is observed. This fast luminescence component does not decay to zero, but levels-off to a constant value that is lower in its magnitude as the concentration of BXV^{4+} increases. In fact, this residuary luminescence appears as a constant value at this short time scale, but corresponds to the slow decaying process of the free photosensitizers that was discussed above. The fast decaying component in the luminescence transients is attributed to the static, intramolecular quenching of the photosensitizer within the supramolecular assemblies formed with
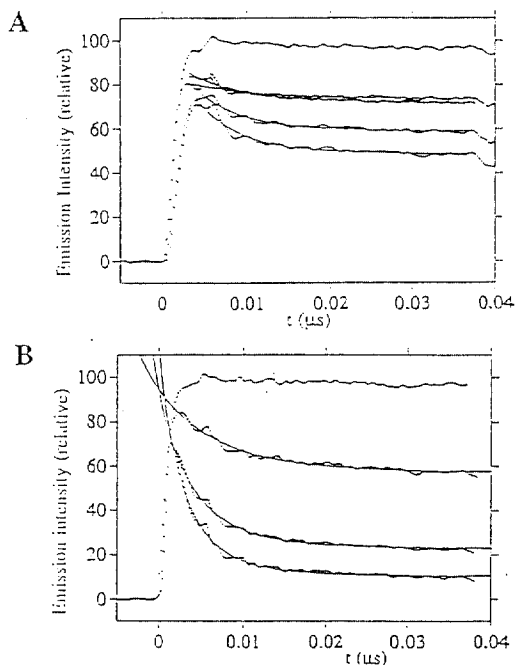
Fig. 8. Decay of the emission intensity of photosensitizers (A) **2** and (B) **3**, within a time scale of a few nanoseconds, in the presence and absence (upper curves) of BXV^{4+}. The transients correspond, from top to bottom in each frame, to BXV^{4+} concentrations: 0 M, 1.7×10^{-3} M, 3.3×10^{-3} M and 5.0×10^{-3} M. Least-squares fitting curves are overlaid on the experimental points.

BXV^{4+}. For photosensitizer (**3**), the contribution of the fast luminescence decaying component is substantially higher than the respective decaying component of (**2**), at the identical BXV^{4+} concentrations. This is consistent with the higher population of the supramolecular complexes in the two-shell photosensitizer, (**3**).

The fast luminescence transients shown in Fig. 8(A) and 8(B) were fitted to Eq. (11) by means of an iterative least-squares fitting program. The term $\exp(k_D + k_{dq}[A])t$ was omitted, since at short time scales it nearly equals unity, and only the parameters $I(0)$, $K[A]$ and k_{sq} were optimized. The fitted curves are overlaid on the experimental transients in Fig. 8(A) and 8(B). For different BXV^{4+} concentrations, nearly identical values for $I(0)$ and k_{sq} are derived, but the $K[A]$ values differ. The derived intramolecular ET-quenching rate constants of (**2**) and (**3**) correspond to $k_{sq} = 1.5 \times 10^8$ s^{-1} and $k_{sq} = 1.7 \times 10^8$ s^{-1}. The extracted association constants of BXV^{4+} to a single π-donor branch of (**2**) and (**3**) correspond to $K = 15 \pm 2$ M^{-1} and $K = 90 \pm 10$ M^{-1} respectively. These values are very similar to those derived from the steady-state luminescence experiments. We also note that the intramolecular static quenching rate constants of the photosensitizers (**2**) or (**3**) by BXV^{4+}, are almost identical, despite the two-shell configuration of the π-donor sites in (**3**). We know from previous studies of photoinduced ET in other octopus-like photosensitizer–acceptor supramolecular assemblies [47] that the rate of static

quenching depends very strongly on the length of the oxyethylene tethering chains, according to Marcus theory, up to a factor of 5 for any additional ethylene glycol unit. Thus, in the present case, BXV^{4+} is located in both complexes at almost identical distances from the photosensitizer center. This is consistent with the formation of a π-stacked assembly of the two dialkoxybenzene units comprising the two-shell complex with BXV^{4+}, Fig. 7. This rigidifies the BXV^{4+} electron acceptor to a distance close to that present in the supramolecular structure between BXV^{4+} and the Ru(II)-center in (2).

2.6. Back ET analysis

The ET products formed by the static and diffusional quenching routes were characterized with respect to their rates of back ET, Eqs. (7) and (8), and the extent of charge separation, Eq. (9). Fig. 9 shows the transient decay of $BXV^{3+\cdot}$ that is formed upon photoexcitation of (3) by the two different quenching routes. The reduced photoproduct $BXV^{3+\cdot}$ exhibits an absorbance band at $\lambda = 600$ nm, characteristic of bipyridinium radical cations. A fast exponential decay corresponding to the back ET within the supramolecular complex, Eq. (8), $k_{sr} = 1.6 \times 10^6 \, s^{-1}$, is observed, followed by a slow decay that follows a second-order kinetics, and corresponds to the diffusional recombination of $BXV^{3+\cdot}$ with the oxidized photosensitizer, $k_{dr} = 4 \times 10^5 \, M^{-1} \, s^{-1}$, Eq. (7). The fraction of $BXV^{3+\cdot}$ that recombines via the diffusional path is $\theta_{dr} = 0.14$. In this context, it is interesting to compare the fraction of $BXV^{3+\cdot}$ that recombines via the diffusional mechanism. The efficiency of diffusional quenching is given by $\theta_{dq} = ([S]/S_o)k_{dq}[A]/k_D + k_{dq}[A])$, where [S] is the concentration of the unbound photosensitizer and S_o is the overall concentration of the photosensitizer. Using Eq. (10), the derived value of k_{dq} and the acceptor concentration at which $BXV^{3+\cdot}$ was recorded, 2.5×10^{-3} M, the ET-quenching efficiency is $\theta = 0.13$.

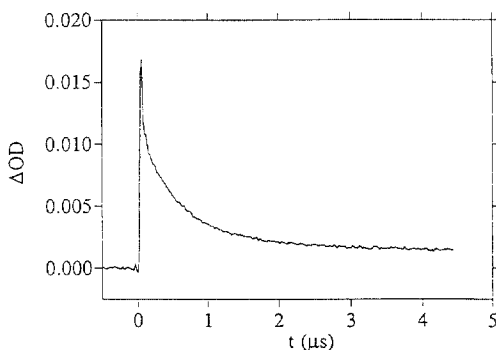This quantitative comparison allows us to conclude that no charge separation

Fig. 9. Transient decay of the absorption of the reduced photoproduct, $BXV^{3+\cdot}$, formed upon excitation of **3** in the presence of BXV^{4+} (2.5×10^{-3} M), as a result of back ET. Reduced photoproduct was followed at $\lambda = 600$ nm.

occurs in the system, $k_{esc} \ll k_{sr}$. The $BXV^{3+\cdot}$ formed by static quenching recombines within the supramolecular assembly without separation. The back ET of $BXV^{3+\cdot}$ that proceeds via the diffusional path, corresponds to the reduced photoproduct that was generated by diffusional ET-quenching. No charge separation of the redox photoproducts generated in the supramolecular complexes takes place. This conclusion has important basic implications, as it demonstrates a novel method to tailor photosensitizer–electron acceptor diads by supramolecular interactions. These photosensitizer–acceptor assemblies stabilized by non-covalent bonds behave as intact diads, whereas ET-quenching and recombination proceed in the supramolecular system. From a practical point of view, the lack of charge separation is disadvantageous, since back ET within the supramolecular complexes is fast. The superior control of the photoinduced ET involves charge separation of the redox-species subsequent to the intramolecular static quenching in the supramolecular complexes. The possible origin of the lack of charge separation in the complexes resulting from the association of BXV^{4+} to the one-shell and two-shell photosensitizers (**2**) and (**3**) is the structure of the electron acceptor. The electron acceptor, BXV^{4+}, consists of two bipyridinium units in a cyclophane structure. Upon reduction to $BXV^{3+\cdot}$, one of the bipyridinium sites is reduced, but the complementary component of bipyridinium exhibits affinity for the π-donor sites. This affinity is low and, therefore, the primary use of the monofunctional N,N'-dialkyl-4,4'-bipyridinium electron acceptor is prohibited, but it influences the charge-separation to the extent that the dissociation of the supramolecular complex is slow compared with the internal back ET.

3. Photoinduced ET in dialkoxybenzene-capped Zn(II)-porphyrin/N,N'-dimethyl-4,4'-bipyridinium supramolecular assemblies

Our discussion suggests that effective control of photoinduced ET in supramolecular assemblies could be accomplished in systems where monofunctional electron-acceptors, such as N,N'-dialkyl-4,4'-bipyridinium, are employed and photosensitizers exhibiting high donor–acceptor binding affinities for the monofunctional electron acceptor are used. Photoreduction of the monofunctional electron acceptor is anticipated to yield a product lacking electron acceptor features, and thus its separation from the supramolecular assembly could be facilitated. This approach was recently materialized [49] with the use of a series of dialkoxybenzene π-donor capped Zn(II)-porphyrins and the monofunctional electron acceptor N,N'-dimethyl-4,4'-bipyridinium hexafluorophosphate, MV^{2+}, (**4**). Specifically, we address here the photoinduced ET in supramolecular assemblies formed between the dialkoxybenzene-capped Zn(II)-porphyrin, (**5**), and MV^{2+}. The photoexcited states for Zn(II)-porphyrins participating in the static and diffusional quenching paths, differ from those discussed for the Ru(II)-polypyridine complexes. Whereas for the Ru(II)-photosensitizers identical photoexcited states are quenched via the intramolecular and diffusional quenching routes, the Zn-porphyrin exhibits two distinct states of different multiplicity states that are active in the ET-quenching pathways.

$$CH_3-N^+ \langle \text{pyridyl} \rangle - \langle \text{pyridyl} \rangle N^+-CH_3 \quad \cdot \; 2\,PF_6^-$$
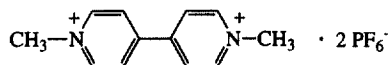
4
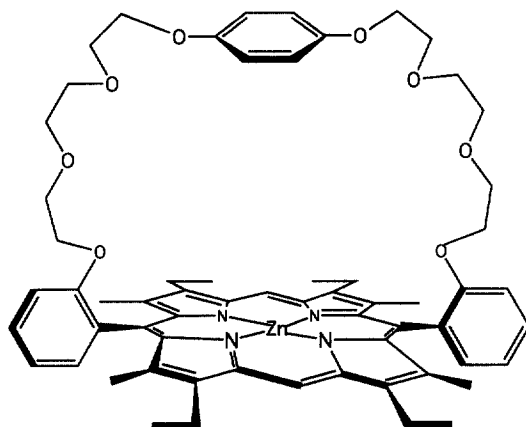
5

3.1. Kinetic model and analysis

Fig. 10 shows the expected scheme of photoinduced ET in the presence of the Zn-porphyrin as photosensitizer. Formation of a π-donor–acceptor supramolecular complex between the dialkoxybenzene unit, capping the Zn-porphyrin, and MV^{2+} yields a supramolecular assembly where the excited singlet state is being quenched
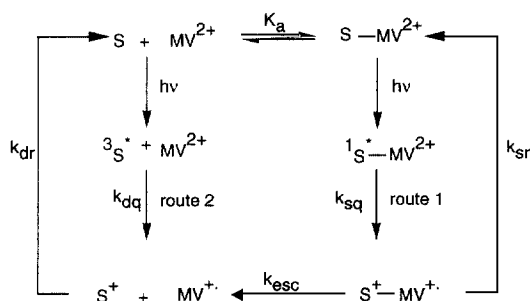
Fig. 10. Kinetic scheme of the photoinduced ET in the system containing the photosensitizer **5** (S) and the electron acceptor MV^{2+}.

to yield the cage structure of photoproducts. The free photosensitizer S is photoexcited to the short-lived singlet that undergoes intersystem crossing to the triplet Zn(II)-porphyrin. This long-lived species undergoes diffusional quenching by MV^{2+}. As the electron acceptor is monofunctional, the photogenerated $MV^{+\cdot}$ lacks affinity for the oxidized photosensitizer, and separation of the intimate pair of redox products can occur and lead to charge separation.

3.2. Time-resolved absorption experiments

Fig. 11 shows the transient decay curves of the excited triplet ^{3}Zn-porphyrin ($\lambda = 470$ nm) in the absence of MV^{2+} and upon increase of the concentration of added MV^{2+}. The natural decay of the ^{3}Zn-porphyrin triplet exhibits a lifetime of 3.6 µs. The intersystem crossing quantum yield from the ^{1}Zn-porphyrin to the triplet is $\theta_{ST} = 0.52$. Addition of MV^{2+} accelerates the triplet decay and decreases the initial concentration of the triplet state in the system. As the MV^{2+} content increases, the amount of triplet generated decreases and its lifetime is shortened. These results are consistent with π-donor-capped Zn-porphyrin and MV^{2+}, and the operation of the static and diffusional ET-quenching processes. Formation of the complex stimulates the static, intramolecular quenching of the singlet state, thereby reducing the yield of the triplet state. The shortening in the triplet lifetime is due to the diffusional quenching of the triplet. Fig. 12 shows the plot of the triplet lifetime as a function of MV^{2+} concentration, according to Eq. (14). The derived diffusional ET-quenching rate constant is $k_{dq} = 5.8 \times 10^9 \, M^{-1} \, s^{-1}$. The association constant of MV^{2+} to the Zn-porphyrin, (**5**), can be elucidated by following the generated triplet concentration at various MV^{2+} concentrations. The triplet concentration in the absence or presence of MV^{2+} relates directly to the concentration of the free photosensitizer, and the decrease in the triplet concentration upon addition of MV^{2+} is due to the formation of the supramolecular assembly that undergoes static quenching. Accordingly, the association constant of the supramolecular complex
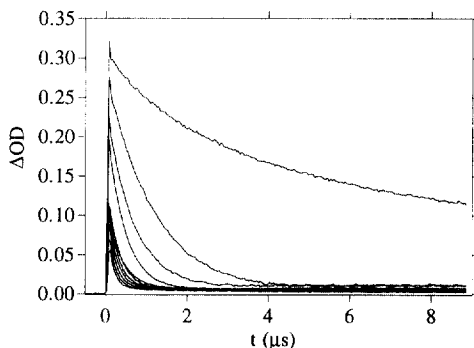

Fig. 11. Time-dependent triplet absorption decay of the photosensitizer **5** (3.6×10^{-5} M) in the presence of increasing concentrations of MV^{2+} ranging from 0 M (upper curve) to 1.0×10^{-4} M (lower curve), by intervals of 10^{-5} M.
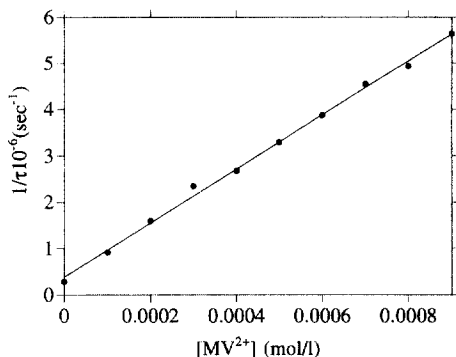
Fig. 12. Triplet lifetime of photosensitizer **5** (3.6×10^{-5} M) at different concentrations of MV^{2+}.

between (**5**) and MV^{2+} can be expressed by Eq. (16), which can be reorganized in terms of Eq. (17). In this relation, $[^3S^*](t=0, [A]=0)$ and $[^3S^*](t=0, [A]_i)$ correspond to the initial triplet concentration in the absence and presence of MV^{2+}, respectively.

$$\frac{[^3S^*](t=0,[A]=0) - [^3S^*](t=0, [A]_i)}{[^3S^*](t=0, [A]_i)} = K_a[A] \tag{16}$$

$$\frac{[^3S^*](t=0, [A]=0)}{[^3S^*](t=0, [A]_i)} = 1 + K_a[A] \tag{17}$$

Fig. 13 shows the analysis of the triplet concentrations obtained at different MV^{2+} concentrations, according to Eq. (17). The derived association constant corresponds to $K_a = 1.6 \times 10^3$ M^{-1}. Thus, even though the photosensitizer includes only one π-donor dialkoxybenzene unit, and the electron acceptor is a monofunctional bipyridinium salt, the resulting supramolecular complex reveals a substantially higher association constant than the complexes formed between the bipyridinium
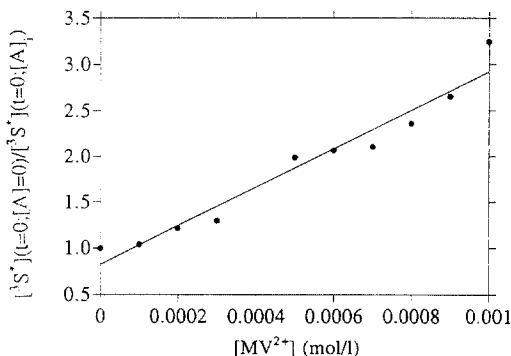

Fig. 13. Plot of the ratio of photosensitizer **5** triplet concentrations in the absence and presence of electron acceptor (A), MV^{2+}, at variable concentrations.

electron acceptor and the Ru(II)-polypyridine series of photosensitizers. In fact, the association constant of (5) to MV^{2+} is ca. 10^2-fold higher than the binding constant of MV^{2+} to a dialkoxybenzene unit tethered to an Ru(II)-photosensitizer ($K_a \approx 30$ M^{-1}). The enhanced affinity for the association of MV^{2+} to the Zn(II)-porphyrin is attributed to the synergetic binding of the electron acceptor to the photosensitizer via complementary modes; in addition to the dialkoxybenzene π-donor site, the Zn(II)-porphyrin moiety provides an additional site for the stabilization of complex with MV^{2+} via π-donor-acceptor interactions. Also, the affinity of MV^{2+} to crown-ethers suggests that the polyoxyethylene bridge that is capping the Zn(II)-porphyrin provides an additional site for the association of MV^{2+} to the photosensitizer. All of these interactions operate synergetically and lead to the high affinity association of MV^{2+} to (5).

3.3. Back ET and charge separation analysis

Finally, we address the formation of photoinduced ET products in the system, the recombination of the ET products and we discuss the possible charge-separation mechanism in the supramolecular assembly consisting of the monofunctional bipyridinium salt. Fig. 14 shows the decay of the photogenerated $MV^{+\cdot}$ ($\lambda = 602$ nm). This follows second-order kinetics and corresponds to the diffusional back ET, Eq. (7), $k_{dr} = 2.8 \times 10^9$ M^{-1} s^{-1}. A closer inspection on the time-dependent evolution of $MV^{+\cdot}$ in the system at a shorter time scale, Fig. 15, reveals some important features. The absorbance of $MV^{-\cdot}$ increases instantaneously upon excitation of the system and then the $MV^{+\cdot}$ follows pseudo first-order kinetics, since the concentration of MV^{2+} is much higher than that of the photosensitizer. Taking into account the concentration of MV^{2+}, the derived second-order rate constant for the formation of $MV^{+\cdot}$ is 7.2×10^9 M^{-1} s^{-1}. This value is similar to the diffusional ET-quenching rate-constant of the triplet state of the photosensitizer. Thus, the time-dependent increase of $MV^{+\cdot}$, Fig. 15, is attributed to its formation by the diffusional ET-quenching route, Fig. 10. The concentration of triplet-generated $MV^{+\cdot}$ via the
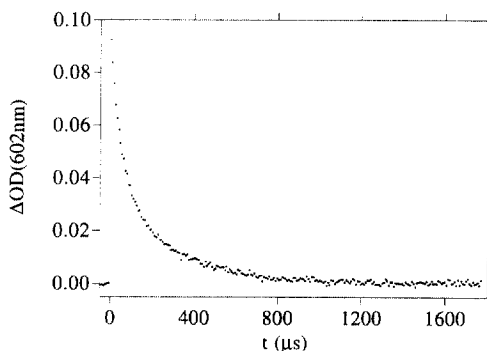

Fig. 14. Time-dependent absorption decay of $MV^{+\cdot}$ (followed at $\lambda = 602$ nm) photogenerated by the excitation of 5 (3.6×10^{-5} M).

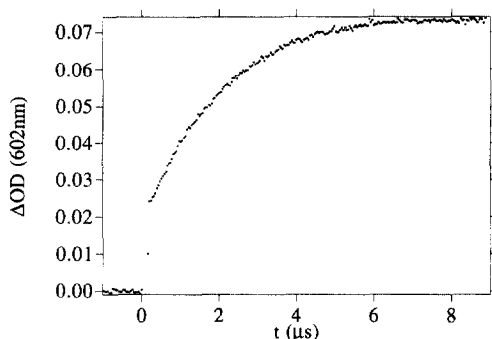Fig. 15. Absorption evolution at $\lambda = 602$ nm upon photoexcitation of the photosensitizer **5** $(3.6 \times 10^{-5}$ M) in the presence of MV^{2+} $(5.0 \times 10^{-5}$ M).

diffusional route is then given by

$$[MV^{+ \cdot}] = \frac{\phi_{ST}[S^*]k_{dq}[MV^{2+}]}{k_D + k_{dq}[MV^{2+}]} \qquad (18)$$

where ϕ_{ST} is the singlet to triplet inter-system crossing quantum yield. The instantaneous increase of the absorbance at $\lambda = 602$ nm, Fig. 15, is attributed to the escape of the singlet-generated $MV^{+ \cdot}$ within the supramolecular assembly by the intramolecular, static quenching route. The instantaneous absorbance increase at $\lambda = 602$ nm originates from the absorbance of escaped $MV^{+ \cdot}$ and a contribution of the absorbance of the triplet photosensitizer. As the concentration of the triplet is known, its absorbance can be subtracted from the observed value at $\lambda = 602$ nm to yield the net absorbance, and hence the concentration, of escaped $MV^{+ \cdot}$, $[MV^{+ \cdot}]_f$. As the concentration of the supramolecular photosensitizer–MV^{2+} complex is known, and since the intramolecular, static quenching can be assumed to proceed quantitatively and convert the supramolecular complex to an intimate redox pair, the escape yield of $MV^{+ \cdot}$ is defined by Eq. (19), where $[S^+ - MV^{+ \cdot}]_o$ is the concentration of the intimate ion pair, or the concentration of the bound photosensitizer.

$$\theta_{esc} = \frac{[MV^{+ \cdot}]_f}{[S^+ - MV^{+ \cdot}]_o} \qquad (19)$$

From the experimental data we calculate a value of $\theta_{esc} \approx 0.45$, i.e. ca. 45% of the $MV^{+ \cdot}$ generated in the supramolecular assembly escapes to yield charge-separated redox species that recombine by a diffusional back ET path.

4. Conclusions

This study has addressed a novel method of assembling supramolecular photosensitizer–acceptor diads via π-donor-acceptor non-covalent interactions. The basic units that lead to the formation of the supramolecular complexes are the dialkoxy-

benzene π-donor component and the N,N'-bipyridinium π-donor-acceptor unit. The π-donor dialkoxybenzene sites were tethered in one-shell and two-shell configurations to a Ru(II)-tris-bipyridine photosensitizer to yield multi-receptor π-donor photosensitizers (2) and (3) respectively. Alternatively, the π-donor dialkoxybenzene site was used as a central receptor-site in capping the Zn(II)-porphyrin photosensitizer, (5). The one-shell and two-shell π-donor, multi-receptor, functionalized Ru(II)-tris-bipyridine photosensitizers (2) and (3) form supramolecular donor–acceptor complexes with the N,N'-bipyridinium cyclophane, BXV^{4+}, (1), where the Zn-porphyrin (5) forms a donor–acceptor complex with N,N'-dimethyl-4,4'-bipyridinium, MV^{2+}, (4). The photoinduced ET in the resulting supramolecular assemblies was characterized by steady-state luminescence quenching studies and time-resolved experiments. A kinetic model that accounts for the features of the photostimulated ET in the supramolecular assemblies was formulated. This enabled us to characterize in detail the association properties of the supramolecular complexes, to elucidate the kinetics of ET in the systems, and to determine the dynamic properties of these non-covalent assemblies.

The π-donor affinity of the dialkoxybenzene site by itself to the monofunctional N,N'-bipyridinium electron acceptor is weak, but can be enhanced by the application of the bipyridinium cyclophane electron acceptor, BXV^{4+}, (1). Further enhancement in the π-donor affinity of dialkoxybenzene sites to BXV^{4+} was achieved by the use of the two-shell π-donor-functionalized photosensitizer (3). In the latter system, the two dialkoxybenzene sites cooperatively participate in the association of BXV^{4+}, by intercalation of the bipyridinium electron acceptor between the π-donor components. A further method to stabilize the supramolecular complexes between the π-donor dialkoxybenzene and the bipyridinium electron acceptor included the application of an ethylene-glycol—dialkoxybenzene-capped Zn-porphyrin photosensitizer. The monofunctional electron-acceptor N,N'-dimethyl-4,4'-bipyridinium, MV^{2+}, (4), forms a high-affinity complex with the dialkoxybenzene-capped Zn-porphyrin, $K_a = 1.6 \times 10^3 \, M^{-1}$, that is stabilized by synergetic cooperative interaction, including π-donor–acceptor interactions between MV^{2+} and the dialkoxybenzene site, π-donor–acceptor interactions with the porphyrin site and association of the electron acceptor to the polyoxyethylene, crown-ether, receptor.

In all of the supramolecular assemblies generated between the π-donor receptor sites and the bipyridinium electron acceptors, effective intramolecular static ET-quenching proceeds. This is accompanied by diffusional ET-quenching of the free photosensitizer. The effectiveness of the static intramolecular ET-quenching is controlled by the number of receptor sites associated with the photosensitizer and the binding constant of the electron acceptor to the receptor sites. The detailed characterization and comparison of the photoinduced ET in the series of the one-shell and two-shell multi-receptor functionalized photosensitizers (2) and (3) reveal that in the two-shell photosensitizer (3), that includes 12 π-donor receptor sites, supramolecular complexes of maximal stoichiometry of six are formed with BXV^{4+}. This has been attributed to the participation of two π-donor dialkoxybenzene sites in the association of a single BXV^{4+}. The high association constant of the supramolecular assembly formed between (3) and BXV^{4+} leads to effective

intramolecular ET-quenching. Owing to the bifunctional structure of the electron acceptor BXV^{4+}, no significant charge-separation accompanies the intramolecular ET. The non-covalently linked photosensitizer–BXV^{4+} systems behave as intact diads where intra-molecular ET-quenching and back ET proceed in the same molecular assembly. Thus, despite the dynamically labile feature of these supramolecular assemblies, no exchange of the complex components and solution species occurs during the lifetime of the photogenerated redox products. With the supramolecular assembly formed between the capped $Zn(II)$-porphyrin, **(5)**, and the monofunctional electron acceptor, MV^{2+}, effective charge-separation accompanies the static intramolecular ET-quenching process, and ca. 45% of the reduced photoproduct, $MV^{+\cdot}$, formed in the complex assembly separates.

Acknowledgements

References

[1] J. Deisenhofer, O. Epp, K. Miki, R. Huber, H. Michel, J. Mol. Biol. 180 (1984) 385.
[2] J. Deisenhofer, O. Epp, K. Miki, R. Huber, H. Michel, Nature 318 (1985) 618.
[3] C.H. Chang, D. Tiede, J. Tang, U. Smith, J. Norris, M. Schiffer, FEBS Lett. 205 (1986) 82.
[4] M. Grätzel (Ed.), Energy Resources Through Photochemistry and Catalysis, Academic Press, New York, 1983.
[5] A. Harriman, M.E. West (Eds.), Photogeneration of Hydrogen, Academic Press, London, 1983.
[6] I. Willner, B. Willner, in: E. Pelizzetti, M. Schiavello (Eds.), Photochemical Conversion and Storage of Solar Energy, Kluwer, Dordrecht, Netherlands, 1991, p. 151.
[7] N.J. Turro, M. Grätzel, A.M. Braun, Angew. Chem. Int. Ed. Engl. 19 (1980) 675.
[8] J.K. Thomas, Chem. Rev. 80 (1980) 283.
[9] P.-A. Brugger, P.P. Infelta, A.M. Braun, M. Grätzel, J. Am. Chem. Soc. 103 (1981) 320.
[10] I. Willner, J.M. Yang, J.W. Otvos, M. Calvin, J. Phys. Chem. 85 (1981) 3277.
[11] I. Willner, J.W. Otvos, M. Calvin, J. Am. Chem. Soc. 103 (1981) 3203.
[12] S.S. Atik, J.K. Thomas, J. Am. Chem. Soc. 103 (1981) 7403.
[13] D. Mandler, Y. Degani, I. Willner, J. Phys. Chem. 88 (1984) 366.
[14] M. Tachiya, J. Phys. Chem. 87 (1985) 5282.
[15] E. Joselevich, I. Willner, J. Phys. Chem. 99 (1995) 6903.
[16] R. Ziessel, J. Hawecker, J.-M. Lehn, Helv. Chim. Acta 69 (1986) 1065.
[17] A.H.A. Tinnemans, T.P.M. Koster, P.H.M.W. Thewissen, A. Mackor, Recl. Trav. Chim. Pays-Bas 103 (1984) 288.
[18] J. Hawcker, J.-M. Lehn, R. Ziessel, Helv. Chim. Acta 69 (1985) 1990.
[19] C. Kutal, A.J. Corbin, G. Ferraudi, Organometallics 6 (1987) 553.
[20] J. Kiwi, M. Grätzel, Nature 281 (1979) 657.
[21] I. Willner, D. Mandler, J. Am. Chem. Soc. 109 (1987) 7884.
[22] I. Willner, D. Mandler, J. Am. Chem. Soc. 111 (1989) 1330.
[23] I. Willner, B. Willner, Top. Curr. Chem. 159 (1991) 153.
[24] I. Willner, B. Willner, in: D.C. Neckers, D.M. Volman, G. von Bünau (Eds.), Advances in Photochemistry, vol. 20, Wiley, New York, 1995, p. 217.

[25] I. Willner, N. Lapidot, A. Riklin, J. Am. Chem. Soc. 111 (1989) 1883.

[26] I. Willner, N. Lapidot, S. Rubin, A. Riklin, B. Willner, in: D. Kamely, A.M. Chakrabarthy, S.E. Kornguth (Eds.), Biotechnology: Bridging Research and Applications, Kluwer, Dordrecht, Netherlands, 1991, p. 341.

[27] I. Willner, E. Zahavy, Angew. Chem. Int. Ed. Engl. 33 (1994) 581.

[28] I. Willner, E. Zahavy, V. Heleg-Shabtai, J. Am. Chem. Soc. 117 (1995) 542.

[29] J.S. Connolly, J.R. Bolton, in: M.A. Fox, M. Chanon (Eds.), Photoinduced Electron Transfer, Part D, Elsevier, Amsterdam, Section 6.2.

[30] L.F. Cooley, C.E.L. Headford, C.M. Elliott, D.F. Kelley, J. Am. Chem. Soc. 110 (1988) 6673.

[31] D. Gust, T.A. Moore, Top. Curr. Chem. 159 (1991) 103.

[32] D. Gust, T.A. Moore, Science 244 (1989) 35.

[33] T.A. Moore, D. Gust, A.L. Moore, R.V. Bensasson, P. Seta, E. Bienvenue, in: V. Balzani (Ed.), Supramolecular Photochemistry, Reidel, Boston, 1987, p. 283.

[34] D. Gust, T.A. Moore, in: V. Balzani (Ed.), Supramolecular Photochemistry, Reidel, Boston, 1987, p. 267.

[35] M.R. Wasielewski, G.L. Gains, III, G.P. Wiederrecht, W.A. Svec, M.P. Niemczyk, J. Am. Chem. Soc. 115 (1993) 10442.

[36] G.M. Sanders, M. van Dijk, A. van Veldhuizen, M.J. van der Plas, J. Chem. Soc. Chem. Commun. (1986) 1311.

[37] M.R. Wasielewski, M.P. Niemczyk, W.A. Svec, E.B. Pewitt, J. Am. Chem. Soc. 107 (1985) 5562.

[38] S.L. Mecklenburg, B.M. Peek, B.W. Erickson, T.J. Meyer, J. Am. Chem. Soc. 109 (1987) 3297.

[39] E. Danielson, C.M. Elliott, J.W. Mesket, T.J. Meyer, J. Am. Chem. Soc. 109 (1987) 2519.

[40] D.G. Johnson, M.P. Niemczyk, D.W. Minsek, G.P. Widerrecht, W.A. Svec, G.L. Gaines, III, M.R. Wasielewski, J. Am. Chem. Soc. 115 (1993) 5692.

[41] H. Kurreck, M. Huber, Angew. Chem. Int. Ed. Engl. 34 (1995) 849.

[42] D. Gust, T.A. Moore, A.L. Moore, S.-J. Lee, E. Bittersmann, D.K. Luttrull, A.A. Rehms, J.M. DeGraziano, J.M. DeGraziano, X.C. Ma, F. Gao, R.E. Belfored, T.T. Trier, Science 248 (1990) 199.

[43] E.H. Yonemoto, Y.I. Kim, R.H. Schmehl, J.O. Wallis, B.A. Shoulders, B.R. Richardson, J.F. Haw, T.E. Mallouk, J. Am. Chem. Soc. 116 (1994) 10557.

[44] L.A. Vermuelen, M.E. Thompson, Nature 358 (1992) 656.

[45] S.B. Ungashe, W.L. Wilson, H.E. Katz, G.R. Scheller, T.M. Putrinski, J. Am. Chem. Soc. 114 (1992) 8717.

[46] E. Zahavy, M. Seiler, S. Marx-Tibbon, E. Joselevich, I. Willner, H. Dürr, D. O'Connor, A. Harriman, Angew. Chem. Int. Ed. Engl. 34 (1995) 1005.

[47] M. Kropf, E. Joselevich, H. Dürr, I. Willner, J. Am. Chem. Soc. 118 (1996) 655.

[48] E. David, R. Born, E. Kaganer, E. Joselevich, H. Dürr, I. Willner, J. Am. Chem. Soc. 119 (1997) 7778.

[49] E. Kaganer, E. Joselevich, I. Willner, Z. Chen, M.J. Gunter, T.P. Jeynes, M.R. Johnston, J. Phys. Chem. 102 (1998) 1159.

[50] I. Willner, Y. Eichen, M. Rabinovitz, R. Hoffman, S. Cohen, J. Am. Chem. Soc. 114 (1992) 637.

[51] H. Kisch, A. Fernandez, Y. Wakatsuki, H. Yamazaki, Z. Naturforsch. 406 (1985) 292.

[52] K. Nakamura, Y. Kai, N. Yasuoka, N. Kasai, Bull. Chem. Soc. Jpn. 54 (1981) 3300.

[53] Y. Usui, H. Misawa, H. Sakuragi, U. Tokumara, Bull. Chem. Soc. Jpn. 60 (1987) 1573.

[54] I. Willner, Y. Eichen, E. Joselevich, J. Phys. Chem. 94 (1990) 3092.

[55] P.L. Anelli, P.R. Ashton, R. Ballardini, V. Balzani, M. Delgado, M.T. Gandolfi, T.T. Goodnow, A.E. Kaifer, D. Philip, M. Pietraszkiewicz, L. Prodi, M.V. Reddington, A.M.Z. Slavin, N. Spencer, J.F. Stoddart, C. Vincent, D.J. Williams, J. Am. Chem. Soc. 114 (1992) 193.

[56] P.L. Anelli, P.R. Ashton, N. Spencer, A.M.Z. Slawin, J.F. Stoddart, D.J. Williams, Angew. Chem. Int. Ed. Engl. 30 (1991) 1036.

[57] P.R. Ashton, B. Odell, M.V. Reddington, A.M.Z. Slawin, J.F. Stoddart, D.J. Williams, Angew. Chem. Int. Ed. Engl. 27 (1988) 1550.

[58] B.L. Allwood, N. Spencer, H. Shahriari-Zavareh, J.F. Stoddart, D.J. Williams, J. Chem. Soc. Chem. Commun. (1987) 1064.

[59] P.R. Ashton, E.J.T. Chrystal, J.P. Mathias, K.P. Parry, A.M.Z. Slawin, N. Spencer, J.F. Stoddart, D.J. Williams, Tetrahedron Lett. 28 (1987) 6367.

[60] J.F. Stoddart, Pure Appl. Chem. 60 (1988) 467.

[61] M.J. Gunter, D.C.R. Hockless, M.R. Johnston, B.W. Skelton, A.H. White, J. Am. Chem. Soc. 116 (1994) 4810.

[62] D.B. Amabilino, P.R. Ashton, A.S. Reder, N. Spencer, J.F. Stoddart, Angew. Chem. Int. Ed. Engl. 33 (1994) 433.

[63] D.B. Amabilino, P.R. Ashton, A.S. Reder, N. Spencer, J.F. Stoddart, Angew. Chem. Int. Ed. Engl. 33 (1994) 1286.